

# CMB ANISOTROPIES, COSMOLOGICAL PARAMETERS AND FUNDAMENTAL PHYSICS: CURRENT STATUS & PERSPECTIVES

François R. Bouchet

*Institut d'Astrophysique de Paris, CNRS, 98 bis Bd Arago, Paris, F-75014, France*

**Abstract.** I describe briefly the Cosmic Microwave Background (hereafter CMB) physics which explains why high accuracy observations of its spatial structure are a unique observational tool both for the determination of the global cosmological parameters and to constrain observationally the physics of the early universe. I also briefly survey the many experiments which have measured the anisotropies of the CMB and led to crucial advances in observational Cosmology. The somewhat frantic series of new results has recently culminated with the outcome of the WMAP satellite which confirmed earlier results, set new standards of accuracy, and suggested that the Universe may have reionised earlier than anticipated. Many more CMB experiments are currently taking data or being planned, with the Planck satellite on the 2007 Horizon poised to extract all the cosmological information in the temperature anisotropies, and foray deeply into polarisation.

## 1 Introduction

As we shall see, the analysis of the CMB temperature anisotropies indicated that the total energy density of the Universe is quite close to the so-called critical density,  $\rho_c$ , or equivalently  $\Omega = \rho/\rho_c \simeq 1$ . We therefore live in a close-to-spatially flat Universe. In agreement with the indications of other cosmological probes the recent results of the CMB satellite WMAP [4] indicate that about 1/3 of that density appear to be contributed by matter ( $\Omega_M = 0.29 \pm 0.07$ ), most of which is dark - i.e. not interacting electromagnetically - and cold - i.e. its primordial velocity dispersion can be neglected. The usual atoms (the baryons) contribute less than about 5% ( $\Omega_B \simeq 0.047 \pm 0.006$ ) [21]. If present, a hot dark matter component does not play a significant role in determining the global evolution of the Universe. While many candidate particles have been proposed for this CDM, it has not yet been detected in laboratory experiments, although the sensitivities of the latter are now reaching the range where realistic candidates may lay. The other  $\sim 60\%$  of the critical density is contributed by a smoothly distributed vacuum energy density or dark energy, whose net effect is repulsive, i.e. it tends to accelerate the expansion of the Universe. Alternatively, this effect might arise from the presence in Einstein's equation of the famous cosmological constant term,  $\Lambda$ . While this global census, surprising as it may be, had been around already for some time (see § 3), the WMAP results have tightened earlier constraints and gave further confidence to the model. These constraints obtained from the analysis of CMB anisotropies arise from - and confirm - the current theoretical understanding of the formation of large scale structures in the Universe, which we now briefly outline.

The spatial distribution of galaxies revealed the existence of these large scale structures (clusters of size  $\sim 5$  Mpc, filaments connecting them, and voids of size  $\sim 50$  Mpc), whose existence and statistical properties can be accounted for by the development of primordial fluctuations by gravitational instability. The current paradigm is that these fluctuations were generated in the very early Universe, probably during an inflationary period; that they evolved linearly during a long period, and more recently reached density contrasts high enough to form bound objects. Given the census given above, the dominant component that can cluster gravitationally is Cold Dark Matter (CDM).

The analysis of the CMB anisotropies also indicate that the initial fluctuations statistics had no large deviations from a Gaussian distribution and that they were mostly adiabatic, i.e. all components (CDM, baryons, photons) had the same spatial distribution. The power spectrum of the "initial conditions" appears to be closely approximated by a power law  $P(k) = \langle |\delta_k|^2 \rangle = A_S k^{n_S}$ , where  $\delta_k$  stands for the Fourier transform of the density contrast ( $P(k)$  is therefore the Fourier transform of the two-point spatial correlation function). The logarithmic slope,  $n_S$ , is quite close to unity ( $n_S = 0.99 \pm 0.04$  from WMAP alone [21]). This shape implies that small scales collapsed first, followed

by larger scales, with small objects merging to form bigger objects. The formation of structures thus appear to proceed *hierarchically* within a “cosmic web” of larger structures of contrast increasing with time.

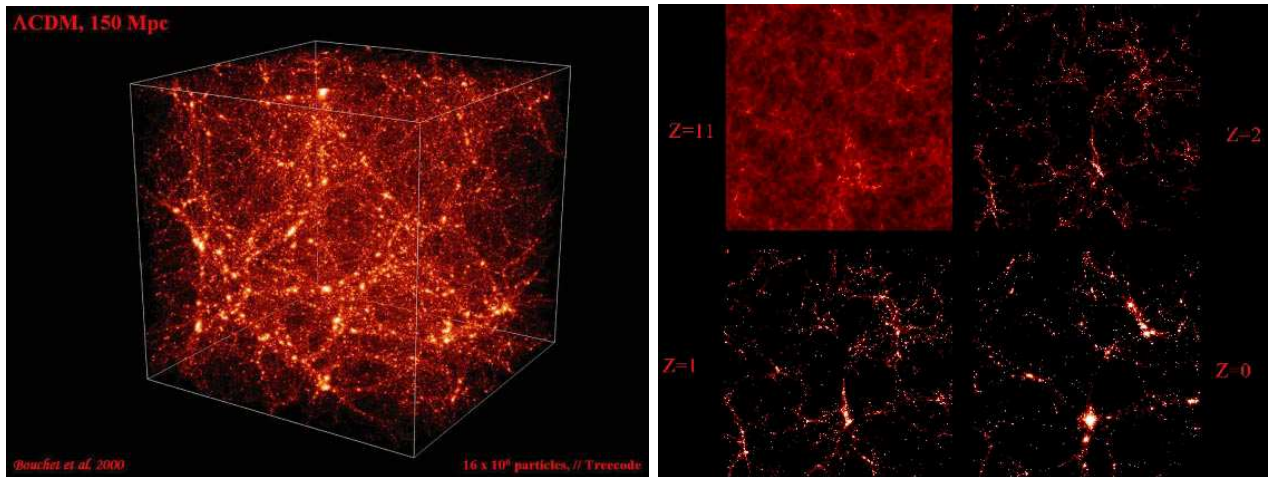


Figure 1: A numerical simulation in a 150 Mpc box of a LCDM Universe ( $\Omega = 1$ ,  $\Omega_\Lambda = 2/3$ ,  $n_S = 1$ ). a) (left) Resulting distribution of the CDM at present (luminosity proportional to the density). b) (right) Temporal evolution by gravitational instability of a thin (15 Mpc) slice of the box showing the hierarchical development of structures within a global cosmic web of increasing contrast, but quite discernible early on.

Figure 1.a shows the generated structures in the CDM components in a numerical simulation box of 150 Mpc, while 1.b shows the evolution with redshift of the density in a thin slice of that box. The statistical properties of the derived distribution (with the cosmological parameters given above) appear to provide a close match to those derived from large galaxy surveys. Note that this simulation with  $\Omega_\Lambda = 2/3$ ,  $\Omega_M = 1/3$  was performed in 2000, well before the WMAP results. Indeed it was already by then the favourite model.

When collapsed objects are formed, the baryonic gas initially follows the infall. But shocks will heat that gas, which can later settle in a disk and cool, and form stars and black holes which can then feed back through ionising photons, winds, supernovae... on the evolution of the remaining gas (after first reionising the Universe at  $z > 6$ ). In this picture, galaxies are therefore (possibly biased) tracers of the underlying large scale structures of the dark matter.

## 2 Physics overview of CMB anisotropies

In this standard cosmological model, processes in the very early universe generate the seed fluctuations which ultimately give rise to all the structures we see today. In the early universe, baryons and photons were tightly coupled through Thomson scatterings of photons by free electrons (and nuclei equilibrated collisionally with electrons). When the temperature in the universe became smaller than about 3000 K (which is much lower than 13.6 eV due to the large number of photons per baryons  $\sim 1.5 \cdot 10^9$ ), the cosmic plasma recombined and the ionisation rate  $x_e$  fell from 1 at  $z > 1100$  down to  $x_e < 10^{-3}$  at  $z < 1100$ : the photons mean free path  $\propto 1/x_e$  rapidly became much larger than the Horizon  $\sim cH^{-1}$ . As a result, the universe became transparent to background photons, over a narrow redshift range of 200 or less. Photons then propagated freely as long as galaxies and quasars did not reionise the universe (but by then the density will have fallen enough that only a small fraction was rescattered). We therefore observe a thin shell around us, the last scattering “surface” (LSS in short) where the overwhelming majority of photons last interacted with baryonic matter, at a redshift of 1100, when the Universe was less than 400 000 years old. The anisotropies of the CMB are therefore the imprint of the fluctuations as they were at that time (but for a small correction due to the photons propagation through the developing Large Scale Structures).

To analyse the statistical properties of the temperature anisotropies, we can either compute the angular correlation function of the temperature contrast  $\delta_T$ , or the angular power spectrum  $C(\ell)$  which is its spherical harmonics transform (in practice, one transforms the  $\delta_T$  pattern in  $a(\ell, m)$  modes and sums over  $m$  at each multipole since the pattern should be isotropic, at least for the trivial topology, in the absence of noise). A given multipole corresponds to an angular scale  $\theta \sim 180^\circ/\ell$ . These two-point statistics characterise completely a Gaussian field. Figure 2.a shows the expected  $C(\ell)$  shape in the context we have described above.

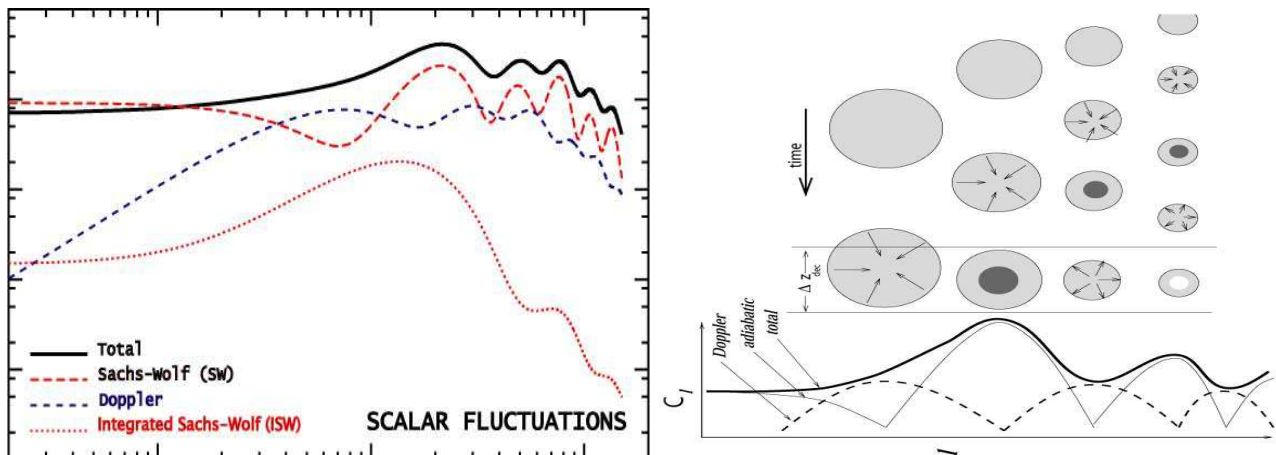


Figure 2: The expected shape of the angular power spectrum of the temperature anisotropies,  $C(\ell)$  (times  $\ell^2$  to give the logarithmic contribution of each scale to the variance). a) Relative contributions; it has been assumed that only scalar fluctuations are present. The plot is in log-log coordinates. b) As time progresses, larger and larger fluctuations start oscillating and leave their characteristic imprint on the spectrum (reprinted from [14]).

This specific shape of the  $C(\ell)$  arises from the interplay of several phenomena. The most important is the so-called “*Sachs-Wolff effect*” [19] which is the energy loss of photons which must “climb out” of gravitational potential wells at the LSS (to ultimately reach us to be observed), an effect which superimposes to the intrinsic temperature fluctuations (we therefore observe an effective temperature which sums this effects, of opposite sign for adiabatic initial conditions where every component [ $\gamma$ , baryons, CDM... ] is perturbed simultaneously). Figure 2.b gives a pictorial view of the temporal development of primordial fluctuations at different scales (top) and how the state of fluctuations translates at recombination in the power spectrum of CMB fluctuations (bottom).

Since the density contrasts of these (scalar) fluctuations is very weak, one can perform a linear analysis and study each Fourier mode independently (the effect of the primordial spectrum will thus simply be to weight the various modes in the final  $C(\ell)$ ). Figure 3 shows the (approximate) temporal evolution of the amplitude of different Fourier modes. While gravity tends to enhance the contrast, the (mostly photonic) pressure resists and at some points stops the collapse which bounces back, and expands before recollapsing again... This leads to acoustic oscillations, on scales small enough that the pressure can be effective, i.e. for  $k > k_A$ , where the acoustic scale  $k_A$  is set by the inverse of the distance travelled at the sound speed at the time  $\eta_*$  considered. On scales larger than the sound horizon ( $k < k_A \propto 1/(c_s \eta_*)$ ), the initial contrast is simply amplified. At  $k = k_A$  the amplification is maximal, while at  $k = 2k_A$  it had time to fully bounce back. More generally, the odd-multiples of  $k_A$  are at maximal compression, while it is the opposite for the even multiples of  $k_A$ .

One should note the displacement of the zero point of the oscillations which results from the inertia that baryons bring to the fluid. The rms of the modes amplitude (right plot) therefore show a relative enhancement of the odd (compression) peaks versus the even (rarefaction) ones, this enhancement being directly proportional to the quantity of baryons, i.e.  $\Omega_B h^2$ , if  $h$  stands for the Hubble “constant”,  $H = \dot{a}/a$ , in units of 100 km/s/Mpc (today  $h_0 = 0.72 \pm 0.05$ ). Note that since  $\Omega_X$  stands for the ratio of the density of  $X$  to the critical density (such that the Universe is spatially flat), and since that critical density decrease with time as  $h^{-2}$ ,  $\Omega_X h^2$  is indeed proportional to the physical density of  $X$ .

Let us assume that the LSS transition from opaque to transparent is instantaneous, at  $\eta = \eta_*$ . What we would see then should just be the direct image of these standing waves on the LSS; one

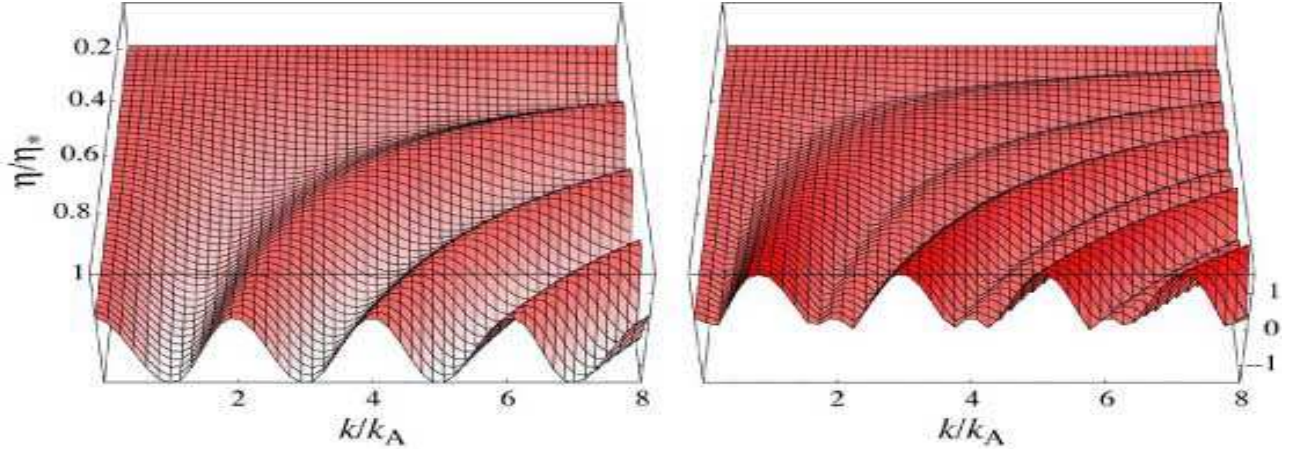


Figure 3: Temporal evolution of the effective temperature which sums the effects (of opposite sign) of the intrinsic temperature and of the Newtonian potential fluctuations (for  $R = (p_B + \rho_B)/(p_\gamma + \rho_\gamma) = \text{cste}$ ). a) (left) Amplitude. Note the zero point displacement which leads to a relative enhancement of compressions. b) (right) rms showing the enhanced odd-numbered peaks. Reprinted from [10].

therefore expects a series of peak at multipoles  $\ell_A = k_A \times D_*$ , where  $D_*$  is the angular distance to the LSS, which depends on the geometry of the spacetime. Of course a given  $k$  contributes to some range in  $\ell$  (when  $k$  is perpendicular to the line of sight, it contributes to lower  $\ell$  than when it is not), but this smearing is rather limited. The dependence of the acoustic angular scale  $\ell_A$  on geometry and sound speed leads to its dependence on the values of three cosmological parameters. One finds for instance

$$\frac{\Delta \ell_A}{\ell_A} \simeq -1.1 \frac{\Delta \Omega}{\Omega} - 0.24 \frac{\Delta \Omega_M h^2}{\Omega_M h^2} + 0.07 \frac{\Delta \Omega_B h^2}{\Omega_B h^2} \quad (1)$$

around a flat model  $\Omega = 1$  with 15% of matter ( $\Omega_M h^2 = 0.15$ ) and 2% of baryons [10]. Note that this information on the peaks positions (and in particular that of the first one) is mostly dependent on the total value of  $\Omega$  (geometry), with some weaker dependence on the matter content  $\Omega_M h^2$ , and an even weaker one on the baryonic density.

Concerning the latter, as already mentioned, baryons increase the inertia of the baryon-photon fluid and shifts the zero point of the oscillations. A larger baryonic density tends to increase the contrast between odd and even peaks; one can therefore use this contrast-in-height information as a baryometer. The influence of dark matter is more indirect. By increasing its quantity, one increases the total matter density and advances the time when matter comes to dominate the energy density of the universe. This changes the duration of time spent in the radiation and matter dominated phase, who may have different growth rates. The net effect is to globally decrease the first peaks amplitude when the matter content increases (in addition to the small shift in scale due to the variation of  $\ell_A$  already noted above). The effect on the power spectrum peaks of all the matter is thus rather different from that of the baryonic component alone. Therefore the shape of the spectrum is sensitive to both separately. This suggests that degeneracies in the effect of these three parameters ( $\Omega, \Omega_M h^2, \Omega_B h^2$ ) can be lifted with sufficiently accurate CMB measurements, a statement which more detailed analyses confirm.

While the reader in a hurry can skip to the conclusion of this section, I now turn to describing other effects which must be taken into account to fully understand the shape of the power spectrum. Since the fluid is oscillating, there is also a *Doppler effect* in the  $k$  direction (blue dotted line in figure 2.a, which is zero at the acoustic peaks and maximal in between. This effect adds in quadrature to the Sachs-Wolf effect considered so far. Indeed, imagine an acoustic wave with  $k$  perpendicular to the line of sight, we see no Doppler effect, while for a  $k$  parallel to the line of sight, the Doppler effect is maximal and the Sachs-Wolf effect is null. This smoothes out the peak and trough structure, although not completely since the Doppler effect is somewhat weaker than the SW effect (by an amount  $\propto \Omega_B h^2$ ). Therefore an increase in the baryonic abundance also increases the peak-trough contrast (in addition to the odd-even peak contrast).

So far we considered the fluid as perfect and the transition to transparency as instantaneous, none

of which is exactly true. Photons scattered by electrons through Thomson scattering in the baryons-photons fluid perform a random walk and diffuse away proportionally to the square root of time (in comoving coordinates which remove the effect of expansion). Being much more numerous than the electrons by a factor of a few billion, they drag the electrons with them (which by collisions drag in turn the protons). Therefore all fluctuations smaller than the diffusion scale are severely damped. This so-called Silk damping is enhanced by the rapid increase of this diffusion scale during the rapid but not instantaneous combination of electrons and protons which leads to the transparency. As a result of the finite thickness of the LSS and the imperfection of the fluid, there is *an exponential cut-off of the large- $\ell$  part* of the angular power spectrum. As a result, there is not much primordial pattern to observe at scales smaller than  $\sim 5'$ .

After recombination, photons must travel through the developing large scale structures to reach the observer. They can lose energy by having to climb out of potential wells which are deeper than when they fell in (depending on the rate of growth of structures, which depends in turn on the cosmological census). Of course the reciprocal is also true, i.e. they can gain energy from forming voids. These tend to cancel at small scale since the observer only sees the integrated effect along the line of sight. The red dotted line of figure 2 shows the typical shape of that *Integrated Sachs-Wolf* (ISW) contribution. The ISW is anti-correlated with the Sachs-Wolf effect, so that the total power spectrum  $C(\ell)$  is in fact a bit smaller than the sum of each spectrum taken separately. Finally, other small secondary fluctuations might also leave their imprint, like the lensing of the LSS pattern by the intervening structures, which smoothes slightly the spectrum. But that can be predicted accurately too. And in fact the smoothing kernel dependence on cosmological parameters introduces small effects that may help reducing some residual degeneracies between the effect of parameters on the power spectrum shape.

Other secondary effects, imprinted after recombination, are generally much weaker (at scales  $> 5'$ ). For instance, the *Rees-Sciama* effect [18] (a non-linear version of the ISW) generates temperature fluctuations, with amplitudes of about a few  $10^{-7}$  to  $10^{-6}$ ; its amplitude is maximum for scales between 10 and 40 arc minutes [20]). At the degree scale, this contribution is only of the order of 0.01 to 0.1% of the primary CMB power. The inverse Compton scattering of the CMB photons on the free electrons of hot intra-cluster gas produces the *Sunyaev & Zeldovich* (SZ) effect [25, 23, 22]). This effect has a specific spectral signature which should allow separating it, at least in sufficiently sensitive multi-frequency experiment. But the motion along the line of sight of clusters induces a first order Doppler effect, usually called the *Kinetic Sunyaev-Zeldovich* effect, which is a true source of temperature fluctuation, albeit rather weak (the rms cluster velocity is  $\sim 10^{-3}c$ ) and in the specific direction of clusters. A similar effect, the *Ostriker-Vishniac effect* [15, 24] arises from the correlations of the density and velocity perturbations along the line of sight, when the universe is totally ionised. The corresponding anisotropies are at the few arc-minute scale and their amplitudes depend much on the ionisation history of the universe [7, 11]). However, they remain smaller than the primary anisotropies for  $\ell < 2000$ . This type of Doppler effect can in fact happen in all sorts of objects containing ionised gas, like expanding shells around the sources that reionised the Universe [2, 9, 13, 3]), or primordial galaxies hosting super-massive black holes [1], but the relevant angular scales are rather in the arc second range or smaller. This does not hold true however for various foreground emission, like those of our own Galaxy. But like for the Sunyaev-Zeldovich effect, one can use multi-frequency observations to separate them out rather well.

In summary, *the seeds of large scale structures must have left an imprint on the CMB, and the statistical characteristics of that imprint can be precisely predicted as a function of the properties of the primordial fluctuations and of the homogeneous Universe*. Reciprocally, we can use measurements of the anisotropies to constrain those properties.

### 3 Observations of CMB anisotropies

Many location have been considered for CMB observations: ground based telescopes at many places in the world, included at South Pole, air-planes, stratospheric balloons, satellites around the Earth, and satellites far from the Earth. The main parameters related to the location are the atmospheric absorption and emission and the proximity of sources of straylight. The Earth atmosphere is a very strong source at millimetre and submillimetre wavelengths [16]. It is therefore a source of photon noise. In addition, it is not perfectly uniform and the slowly changing structure of its emission adds noise that can be confused with CMB anisotropies. Even at stratospheric balloon altitudes (38 to 40 km), one may encounter structures at low angular frequencies that limit measurement stability. Only

satellites are free of this first “layer” of spurious emission.

Straylight coming from the Earth is a common problem for all locations except for space probes distant from the Earth as seen from the instrument. The brightness temperature of about 250K of the Earth times its solid angle has to be compared with the instrument sensitivity in brightness times the beam solid angle. For a mission in low earth orbit the ratio is  $6 \times 10^{13}$  and at the L2 Lagrange point the ratio is  $5 \times 10^9$ . At the wavelengths of interest, diffraction is a major source of straylight, and modelling and experimentation can hardly estimate reliably or measure the very low side lobes needed to meet this extremely high rejection ratio. The problem is severe enough to have motivated the choice of the Lagrangian point L2 of the Sun-Earth system, at about 1.5 million kilometres from Earth, to locate the new generation of satellites WWMAP and PLANCK.

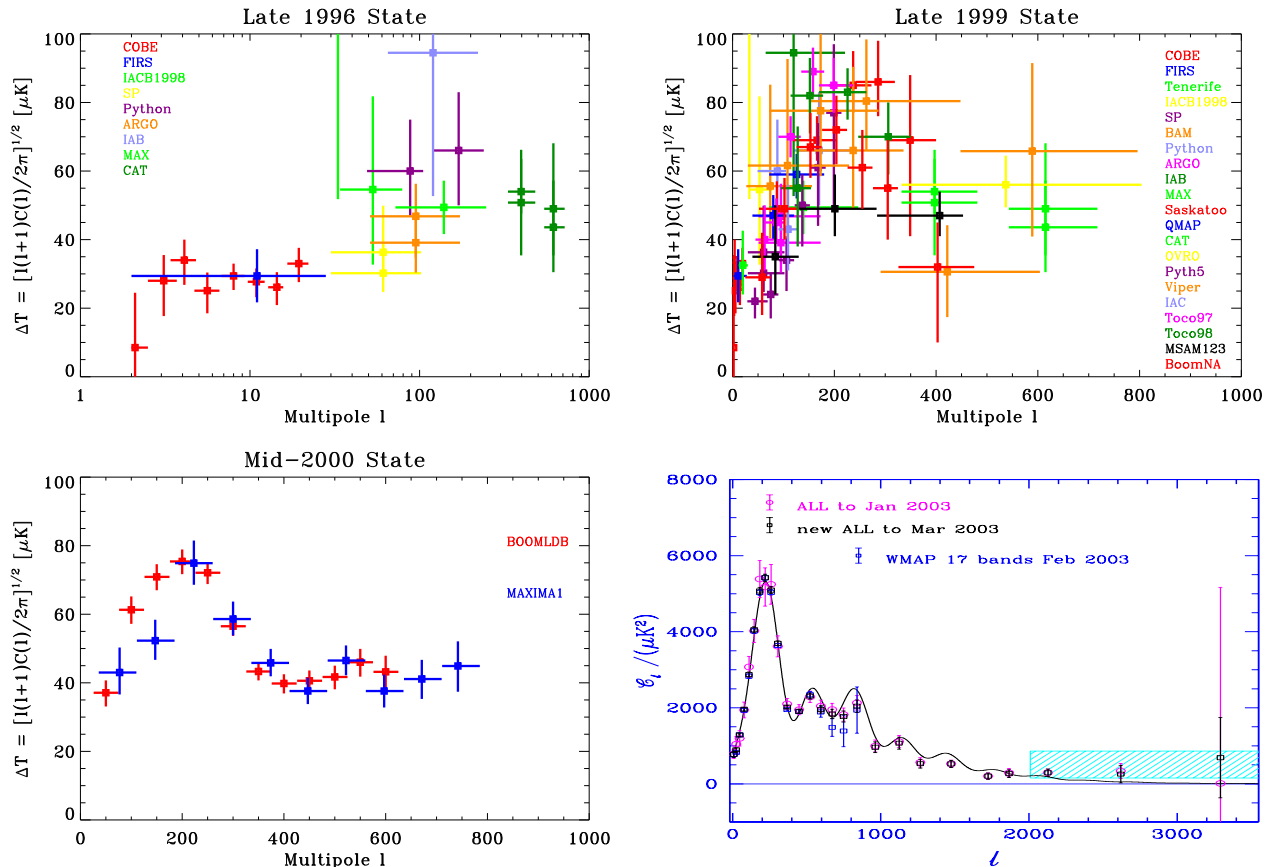


Figure 4: Successive Measurements of the power spectrum. The first panel at top left shows all published detection at the end of 1996, while the second plot at right is an update at the end of 1999. The left bottom plot shows the two results published in may 2000 by the BOOMERanG and MAXIMA teams (with each curve moved by  $+$  or  $- 1 \sigma$  of their respective calibration). The final panel at bottom left (courtesy D. Bond) shows in purple the optimal spectra in 26 bands (allowing for calibration errors in each experiment) from the co-analysis of all data (including Archeops, the extended VSA, ACBAR and a preliminary version of the 2 year CBI data) till January 2003, as well as the WMAP spectrum (blue points), and the spectrum as we know it today (black points) when all experimental evidence are used.

The first clear detection of the CMB anisotropies was made in 1992 by the DMR experiment aboard the COBE satellite orbiting the earth with the DMR instrument (and soon afterwards by FIRS), with a ten degree (effective) beam and a signal to noise per pixel around 1. This lead to a clear detection of the large scale, low- $\ell$ , Sachs-Wolf effect, the flatness of the curve (see fig. 4.a) indicating that the logarithmic slope of the primordial power spectrum,  $n_S$ , could not be far from one. The  $\sim 30\mu\text{K}$  height of the plateau gave a direct estimate of the normalisation of the spectrum,  $A_S$  (assuming the simplest theoretical framework, without much possible direct checks of the other predictions given the

data)

In the next four years (fig 4.a), a number of experiments started to suggest an increase of power around the degree scale, i.e. at  $\ell \sim 200$ . As shown by fig 4.b, by 1999 there was clear indication by many experiments taken together that a first peak had been detected. But neither the height nor the location of that peak could be determined precisely, in particular in view of the relative calibration uncertainties (and possible residual systematics errors).

That situation changed in may 2000 when the BOOMERanG and Maxima collaborations both announced a rather precise detection of the power spectrum from  $\ell \sim 50$  to  $\ell \gtrsim 600$ . That brought a clear determination of the first peak around an  $\ell$  of 220 (see panel c), with the immediate implications that  $\Omega$  had to be close to one. This result had considerable resonance since it clearly indicated, after decades of intensive work, that the spatial geometry of the Universe is close to flat, with of course the imprecision due to the poor determination of the other parameters which also have an influence, albeit weaker, on the position of that peak (see eq. 1).

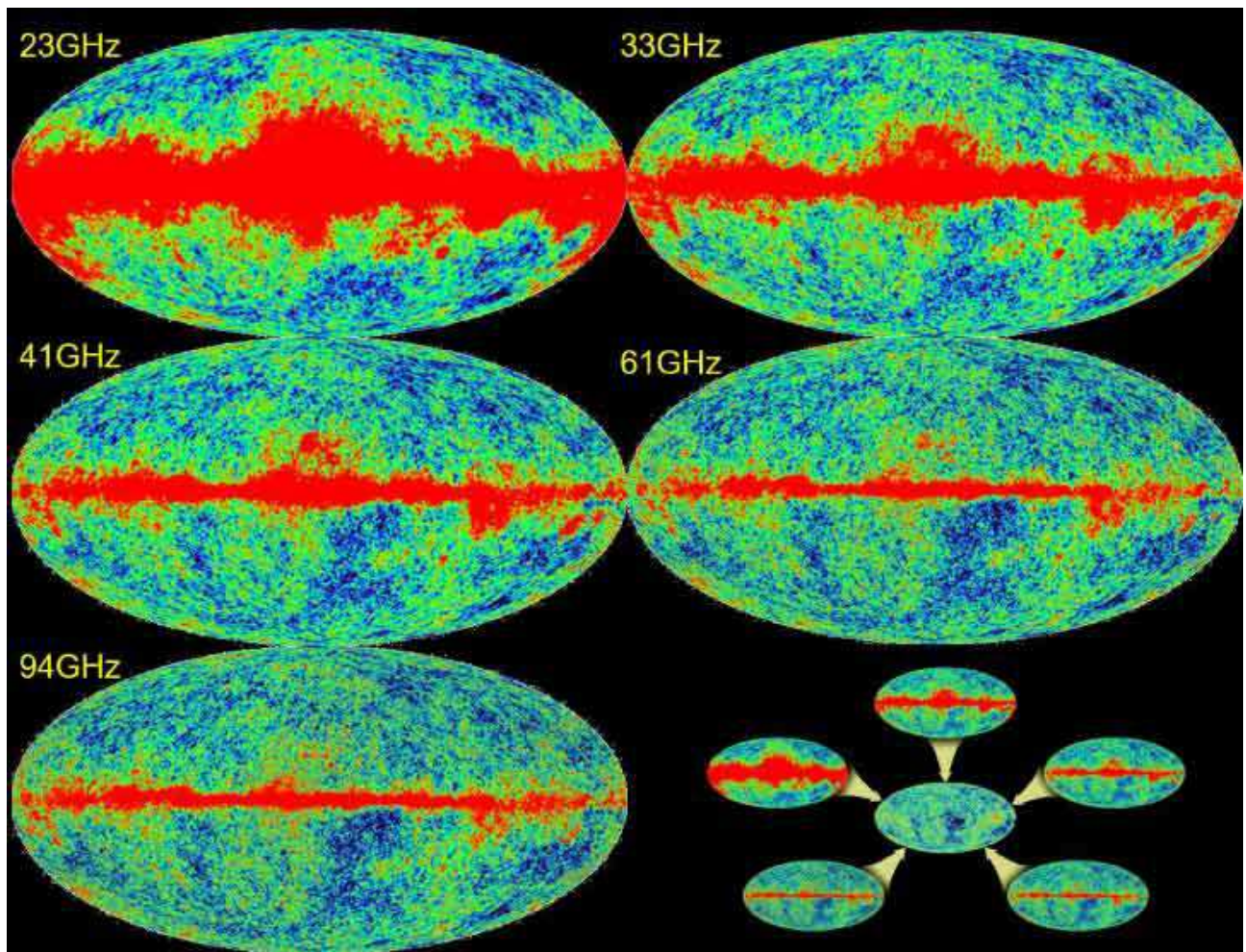


Figure 5: The WMAP maps at each frequency, which shows in particular the varying strength of the Galactic emissions according to frequency, and in the bottom right an icon illustrating that these informations are merged to extract an estimate of the CMB part.

As recalled earlier, a crucial prediction of the simplest adiabatic scenario is the existence of a series of acoustic peaks whose relative contrast between the odd and even ones gives a rather direct handle on the baryonic abundance. In addition, one expects to see at larger  $\ell$  the damping tail. All of these have now been established by the DASI 2001 experiment, an improved analysis of BOOMERanG, and foremost by the release in may of 2002 of the VSA and CBI results. In addition the Archeops experiment gave at the end of 2002 a quite precise determination of the low- $\ell$  part of the spectrum. Panel d of fig 4 shows a co-analysis performed by D. Bond of all results obtained till the end of 2002, as well as the recent determination by the WMAP satellite. Clearly all the pre-WMAP ground

experiments had done quite a wonderful job at pinning down the shape of the temperature spectra. This panel also shows the spectrum as we know it today, when all experimental results are analysed together.

The figure 6 shows the constraints successively posed by these CMB experiments on some of the parameters of the model, using only weak priors arising from other cosmological studies. This priors state that the current Hubble “constant”,  $H_0 = 100h^{-1}\text{km/s/Mpc}$ , has to have a value between 45 and 90 km/s/Mpc, that the age of the Universe has to be greater than 10 Billion years and that the matter density is larger than 1/10 of the critical density, all of which can be considered as very well established (if for instance the Universe has to be older than it’s oldest stars!).

The top left panel shows that indeed that the curvature term  $\Omega_k = 1 - \Omega$  has to be close to zero. The panel on the right shows that  $\Omega_\Lambda$  and  $\omega_c = \Omega_{CDM}h^2$  are not well determined independently of each other by single experiments. This simply reflects the fact that the  $C(\ell)$  global pattern scales by the angular distance (recall  $\ell_A = kAD_*$ ) which is determined by the geometry (i.e.  $\Omega = \Omega_\Lambda + \Omega_{CDM} (+\Omega_B)$ ), while the data is not precise enough to uncover the subtler effects (sound speed, lensing,..) which break that degeneracy. But this degeneracy was lifted by the co-analysis, even before WMAP, and independently of the supernovae result. . .

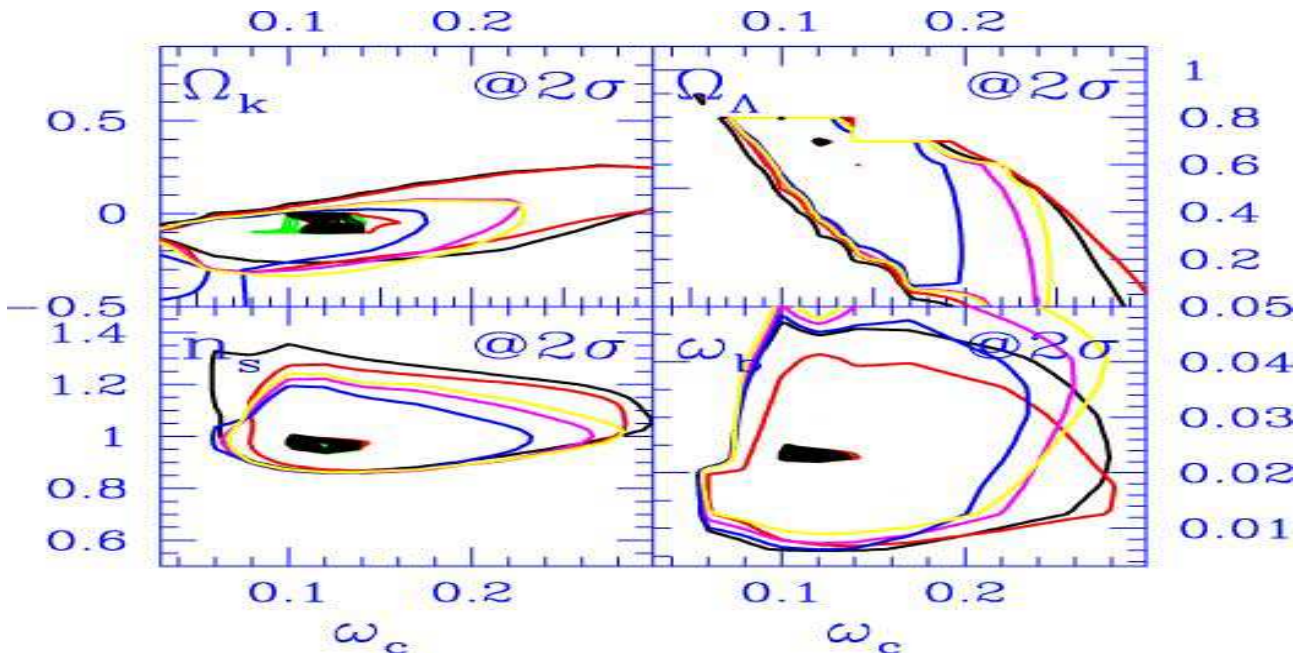


Figure 6: Successive constraints in the  $\Omega_k = 1 - \Omega, \Omega_\Lambda, n_s, \omega_B = \Omega_B h^2$  versus  $\omega_c = \Omega_{CDM} h^2$  cuts in the global parameter space fitted to the  $C(\ell)$  successive data, using COBE/DMR in all cases. The colour coding is the following: CBI = black, VSA = (outer) red, Archeops = yellow, ACBAR = blue, Ruhl cut for Boomerang = magenta. Green corresponds to Acbar + Archeops + Ruhl + DASI + Maxima + VSA + CBI. The interior red is all of the above + WMAP with no prior on  $\tau$ , while black is with a  $\tau$  prior motivated by their “model independent” result from the TE analysis (it is broader than a  $0.16 \pm 0.04$  Gaussian). (Courtesy D. Bond)

The bottom left panel lends support to the  $n_s = 1$  hypothesis. Many inflationary models suggest value of  $n_s$  slightly lower than one (and even departures from a pure power law), but the data is not yet good enough to address these questions convincingly. Completing the census, the bottom right shows the contours in the  $\omega_b - \omega_c$  plane. The CMB determination turns out to be in excellent agreement with the constraints from primordial nucleosynthesis calculations which yield  $\omega_b = \Omega_B h^2 = 0.019 \pm 0.002$ .

In summary, this shows that many of the theoretical predictions corresponding to the simplest scenario for the generation of initial conditions (Gaussian statistics, adiabatic modes, no tensorial contribution, a scale invariant power spectrum) in a flat Universe dominated by dark energy and cold dark matter have now been detected, from the Sachs-Wolf plateau, to the series of peaks starting at  $\ell \simeq 220$ , to the damping tail, together with a first detection of the CMB polarisation at the expected level. The derived parameters are consistent with the various constraints from other cosmological



probes and there are no glaring signs of inconsistencies. This was in fact in place before the WMAP results, but it is remarkable that adding WMAP essentially zooms-in onto the expected values, bringing now further support to the model and its parameters, as recalled in § 1.

## 4 Perspectives

Cosmology therefore has a great *concordance* model, based on a minimal 7 parameters set ( $\Omega, \Omega_{CDM}, \Omega_B, H, \tau$  to describe the global evolution, and  $n_S, A_S$  to describe the initial conditions) which fits quite well all (multiple and partially independent) observational evidence. But it might be too early to consider we have definitively established the *standard* cosmological model, corroborated by many independent probes.

In order to check the strength of the edifice, let us for instance consider what it takes to stick to a simpler Einstein-de Sitter model (EdS, with  $\Omega_{Matter} = 1, \Omega_\Lambda = 0$ ) with no dark energy. As a matter of fact, Blanchard et al. find in [5] a great fit to the currently measured  $C(\ell)$  and a quite reasonable one to the  $P(k)$ , provided they assume that 1) initial conditions are not scale invariant (the authors consider an initial spectrum with 2 slopes) 2) there exists a non-clustering component  $\Omega_x = 0.12$ , both of which are quite possible. The Supernovae data would then be the only source of independent evidence for a non-zero  $\Omega_\Lambda$ , and many would question accepting the existence of such a theoretically-unsettling component on that basis. But this particular Einstein de Sitter model does require also that  $H_0 \sim 46$  km/s/Mpc. This would require in turn that the HST measurement of  $H_0 = 72 \pm 8$  km/s/Mpc be completely dominated by an as-yet unknown systematics effect, which most cosmologists are not ready to accept easily. Accepting this model would thus require discarding two independent line of evidence.

In addition we may now have some rather direct evidence of the presence of dark energy (meaning here  $\Omega_\Lambda \neq 0$ ). Indeed, Bough & Crittenden [6] and Fosalba & Gaztanaga [8] found a significant cross-correlation between the CMB anisotropies measured by WMAP and various tracers of Large Scale Structures. This was anticipated since the evolution of potential wells associated to developing large scale structures when CMB photons travel through them generally leaves an imprint, which we already described, the Integrated Sachs-Wold effect (ISW). This imprint must of course be correlated with tracers of LSS. It is interesting to note that, in the EdS model, gravitational potential wells are linearly conserved in the matter era, in which case no correlation should be found. Instead Bough & Crittenden [6] found a non-zero value at the  $2.4$  to  $2.8\sigma$  level at zero lag of the cross-correlation function of the WMAP map data with the hard X-Ray background measured by the HEAO-1 satellite. They also found a somewhat less significant correlation (at the  $1.8$  to  $2.3\sigma$  level) with an independent tracer, the radio counts from the NVSS catalogue. Fosalba & Gaztanaga [8] used instead the APM galaxy catalogue to build the (projected) density field by smoothing at  $5.0$  &  $0.7$  degree resolution and they also found a substantial cross-correlation. . . While these detections may not yet be at a satisfactory level of significance for such an important implication, it does bring a third line of evidence against the model proposed in [5].

Let us therefore assume that this concordance model offers at least a good first order description of the Universe. Still, deviations from this minimal description remain quite possible and interesting. One possibility much debated recently is that what appears to be the manifestation of a cosmological constant be rather a dynamical entity, for instance a quintessence field with an equation of state where the pressure to density ration is equal to  $w(z)$  (the cosmological constant corresponding to the case  $w = -1$ ). Another possibility concerns a small contribution from massive neutrinos. In both cases better CMB data might help determine these effects. But the domain where most progress is expected and eagerly awaited concerns the characterisation of initial conditions and its implications for physics of the Early Universe. I now turn to a brief overview of various type of deviations that future CMB observations might unearth or constrain much more strongly.

Till now, we only considered *scalar* (adiabatic) fluctuations. Vectorial perturbations tend to decay with expansion and are not predicted to leave any imprint on the spectrum. But it is anticipated that that the very same process that generated the primordial scalar fluctuations also created a stochastic background of gravity waves. This weak tensorial contribution only appears in the low- $\ell$  part of the temperature anisotropies spectrum, before the first peak (since these waves decay as soon as there wavelength becomes smaller than the horizon, which roughly corresponds in  $\ell$  to the first peak). At the current level of experimental precision it is most often ignored. But this contribution is (relatively) much more significant for the polarised part of the emission to which we now turn.

Thomson scatterings can create polarisation provided the incident radiation is not isotropic, which can be induced by velocity gradients in the baryon-photon fluid. Before recombination, successive scatterings destroy the build up of any polarisation. One therefore anticipates a small degree of polarisation created *at* recombination, partially correlated with the temperature anisotropies (the velocity part of it). It is convenient to decompose the polarisation field into two scalar fields denoted E and B (to recall the similarity of their parity properties with that of the electromagnetic fields). The power spectrum of the E part is expected to be about 10 times smaller than for the temperature field T, and the B part *which is only generated by tensor fluctuations* (and by lensing of the CMB by foreground structures) is yet weaker. The WMAP team did not release so far a measurement of the EE power spectrum, but did provide a measurement of the T-E cross power spectrum which quantifies the expected correlation of the temperature and E field.

The WMAP TE spectra turned out to be unexpectedly large at very-low- $\ell$ , which gave strong evidence that the optical depth to the last scattering surface is rather important ( $\sim 0.17$ ), suggesting that reionisation happened rather early, around  $z \simeq 17$  in typical models. One should note that this TE spectrum is easier to measure than the EE one owing to the much larger signal to noise of the temperature, and the cancellation of errors in a cross-correlations. But if at WMAP sensitivities the TE and EE spectra carry equal weight (e.g. for constraining the reionisation history), at higher sensitivity all the information comes from EE. In any case, the important point to note is that polarisation measurements of the CMB simply probe various aspects of the same physics that gave rise to the temperature anisotropies. Such measurements will therefore offer a way to check the internal consistency of the CMB measurements and help remove degeneracies present when temperature alone is considered.

More importantly, polarisation measurements will provide the best way to constrain the scalar to tensor to scalar ratio,  $r = A_T/A_S$  (of the normalisations of the primordial perturbations spectra). Sufficiently sensitive measurements will then allow checking the consistency relation between  $r$  and the logarithmic slope of the gravitational wave power spectrum,  $n_T$ , which is predicted for inflation. Currently we can only say that  $r < 0.71$  at 95% confidence limit [21], if only CMB data with no further priors are used, with essentially no constraint on  $n_T$ , but the data will undoubtedly continue to improve. Indeed fig. 7 shows the current constraints set by WMAP in the  $(r, n_s)$  plane, as well as a forecast for PLANCK.

So far we concentrated on the case of *adiabatic* perturbations which develop under their own gravity when they are much larger than the horizon. After they enter the horizon, they become gravitationally stable and oscillate. All perturbations of the same scale are in phase and started oscillating (for a given wavelength) at the same time. These leads to the so called acoustic peaks in the resulting CMB power spectrum. In the case of active source of fluctuations like in defects theories, perturbations are laid down at all times, they are generically isocurvature (i.e. it's only the relative abundance of the fluid components that vary), non-Gaussian, and the phases of the perturbations of a given scale are incoherent, which does not lead to many oscillation like in the coherent (*e.g.* inflationary) case. A single broad peak is expected, and this is why current CMB anisotropy data already indicates that defects cannot be a major source of CMB fluctuations and hence cannot seed by themselves the growth of the large scale structures of the Universe. Still the current CMB data does not yield strong constraints on which fraction of the perturbations could be isocurvature in nature (Gaussian or not), while many early universe realistic models naturally lead to the production of some isocurvature modes. A determination of such fluctuations, or much tighter upper limit would therefore be extremely valuable.

Finally one should stress that even if one assumes purely adiabatic initial conditions, the current data does not allow yet to put strong constraints on possible deviations from a pure power-law, while measured deviations would have far-reaching consequences.

One anticipates that the rapid pace of advances from CMB observations will remain unabated, since the WMAP team should announce its second data release in early 2004, it is already known that the BOOMERANG Polarization flight of January 2003 was a success and the analysis should not be much longer than a year. In addition, lots of exciting ground and balloon experiments are under development. Finally, the Planck satellite from ESA is poised for launch in 2007. In order to give an idea of the progresses expected in the next few years, I now turn to a WMAP/Planck comparison.

## 5 Planck satellite

The global similarities and differences of WMAP and PLANCK are the following:

- Both map the full sky, from an orbit around the Lagrangian point L2 of the Sun-Earth system, to minimise parasitic radiation from Earth. Both are based on the use of off-axis Gregorian telescopes in the 1.5m class. And very importantly for CMB experiments, both do highly redundant measurements to better detect and remove (or constrain residuals of) possible systematics effect, thanks to the long duration of the data taking (at least a year, to be compared with at most about 10 days for ground experiments which have to cope in addition with the effect of a changing atmosphere - like ozone clouds, the closeness to earth, etc...). And both aim at making polarisation measurements.
- The American WMAP has been designed for rapid implementation, and is based on fully demonstrated solutions. It's observational strategy uses the differential scheme. Two telescopes are put back to back and feed differential radiometers. These radiometers use High Electronic Mobility Transistors (HEMTs) for direct amplification of the radio-frequency (RF) signal. Angular resolutions are not better than 10 minutes of arc.
- The European PLANCK is a more ambitious and complex project, which is to be launched in 2007. It is designed to be the ultimate experiment in several respects. In particular, several channels of the High Frequency Instrument (HFI) will reach the ultimate possible sensitivity per detector, limited by the photon noise of the CMB itself. Bolometers cooled at 0.1 K will allow reaching this sensitivity while, simultaneously, improving the angular resolution to 5 minutes of arc. The Low Frequency Instrument (LFI) limited at frequencies less than 100GHz, will use HEMT amplifiers cooled at 20 Kelvin to increase their sensitivity. The PLANCK scan strategy is of the total power type. The LFI uses 4K radiative loads for internal references to obtain this total power measurement. The HFI readout scheme is based on an electric modulation of the detector allowing total power measurement. The combination of these two instruments on PLANCK is motivated by the necessity to map the foregrounds in a very broad frequency range: 30 to 850 GHz.

More quantitative aspects are detailed in Table 1, although these are only indicative since design evolve and in-flight performance may differ from the requirements (in good or bad, either way are possible).

Table 1: *Planck instrument characteristics. The sensitivities ( $1\sigma$ ) are goal values for 12 months integration and for square pixels whose sides are given in the row "Angular Resolution". Polarisation measurement at 100 GHz on HFI is waiting for approval (the sensitivity level without polarisation measurement at 100 GHz is given in parenthesis).*

Detector Technology	LFI			HFI					
	HEMT arrays			Bolometer arrays					
Center Frequency [GHz]	30	44	70	100	143	217	353	545	857
Number of Detectors	4	6	12	8 (4)	12	12	6	8	6
Bandwidth ( $\Delta\nu/\nu$ )	0.2	0.2	0.2	0.33	0.33	0.33	0.33	0.33	0.33
Angular Resolution (arcmin)	33	241	14	9.2	7.1	5.0	5.0	5.0	5.0
$\Delta T/T$ per pixel (Stokes I) [ $\mu K/K$ ]	2.0	2.7	4.7	2.5 (2.2)	2.4	3.8	15	17	8000
$\Delta T/T$ per pixel (Stokes Q and U) [ $\mu K/K$ ]	2.8	3.9	6.7	4.1 (NA)	4.8	7.6	30	...	...

In order to illustrate how this translates in terms of constraints on early Universe physics, figure 7.b compares the current WMAP  $2\sigma$  constraints (light blue area) versus that anticipated from PLANCK (white area), in the plane ( $r, n_S$ ), where  $r$  stands for the amplitude of the primordial tensorial (gravitational wave) power spectrum in units of the amplitude of the primordial scalar (curvature) power spectrum, and  $n_S$  stands for the logarithmic slope of the primordial scalar spectrum (at some scale). Each black dot corresponds to a couple of reasonable inflation parameters [12]. In the region of overlap of the dots cloud with the WMAP-allowed region, the four colour overlays (red, green, purple and black) each correspond to a particular class of inflation models ranked by curvature of the potential [17]. As extraordinary as it is to start constraining those elusive but fundamental parameters, it

remains that nearly every inflation model class is still alive today. But as the white area shows, the Planck data should allow “zooming-in” on the parameters of the specific model which will be selected by the data (if there is such a model, i.e. if the spectra data does not force us to start considering a broader class than single field slow-roll models).

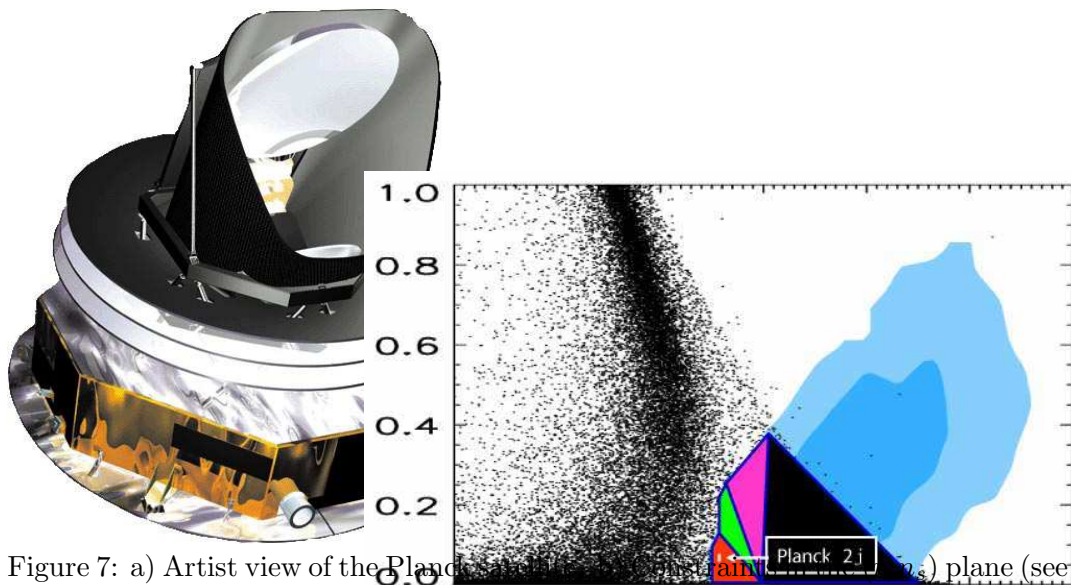


Figure 7: a) Artist view of the Planck satellite. b) A scatter plot of inflation parameters. Each black dot corresponds to 2 parameters of a single field slow-roll inflation models with valid dynamics [12]. The blue shaded regions corresponds to the 1 and  $2\sigma$  constraints from WMAP [17], with the red green purple and black overlays each delimiting a class of inflation model (see text). The white area illustrate the type of accuracy expected from PLANCK, namely  $\Delta r \simeq \Delta n_s \simeq 0.02$ .

c

Before concluding that section, we should recall that the power spectra are only a first moment (the transform of a 2-pt angular correlation function). While enough to characterise a fully Gaussian distribution, deviations from Gaussianity *are* expected, albeit at a rather low level. Such a detection would reveal much about the mechanisms at work in the early Universe (if they are not residual systematics...).

## 6 Conclusions

Measurements of the CMB are quite unique in the ensemble of astrophysical observations that are used to constrain cosmological models. They have the same character as fundamental physics experiments; they relate fundamental physical parameters describing our world to well specified signatures which can be predicted before hand with great accuracy.

The knowledge of CMB anisotropies has literally exploded in the last decade, since their momentous discovery in 1992 by the DMR experiment on the COBE satellite. Since then, the global shape of the spectrum has been uncovered thanks to many ground and balloon experiments and most recently the WMAP satellite, so far confirming the simplest inflationary model and helping shape our surprising view of the Universe: spatially flat, and dominated by dark energy (or  $\Lambda$ ) and cold dark matter, with only a few per cent of atoms. But the quest is far from over, with many predictions still awaiting to be checked and many parameters in need of better determination.

If the next 10 years are as fruitful as the past decade, many cosmological questions should be settled, from a precise determination of all cosmological parameters to characteristics of the mechanism which seeded the growth of structures in our Universe, if something even more exciting than what is currently foreseen does not surge from the future data...

## References

- [1] N. Aghanim, C. Balland, and J. Silk. Sunyaev-Zel'dovich constraints from black hole-seeded proto-galaxies. *A&A*, 357:1–6, May 2000.
- [2] N. Aghanim, F. X. Desert, J. L. Puget, and R. Gispert. "Ionization by early quasars and cosmic microwave background anisotropies". *A&A*, 311:1–11, July 1996.
- [3] N. Aghanim, F. X. Desert, J. L. Puget, and R. Gispert. "erratum: Ionization by early quasars and cosmic microwave background anisotropies". *A&A*, 341:640+, Jan. 1999.
- [4] C. L. Bennett, M. Halpern, G. Hinshaw, N. Jarosik, A. Kogut, M. Limon, S. S. Meyer, L. Page, D. N. Spergel, G. S. Tucker, E. Wollack, E. L. Wright, C. Barnes, M. R. Greason, R. S. Hill, E. Komatsu, M. R. Nolta, N. Odegard, H. V. Peiris, L. Verde, and J. L. Weiland. "first year wilkinson microwave anisotropy probe (wmap) observations: Preliminary maps and basic results. *Astrophys. J., in press & astro-ph/0302207*, 2003.
- [5] A. Blanchard, M. Douspis, M. Rowan-Robinson, and S. sarkar. An alternative to the cosmological "concordance model". *astro-ph/0304237*, 2003.
- [6] S. Boughn and R. Crittenden. A correlation of the cosmic microwave sky with large scale structure. *astro-ph/0305001*, 2003.
- [7] S. Dodelson and J. M. Jubas. "reionization and its imprint of the cosmic microwave background". *ApJ*, 439:503–516, Feb. 1995.
- [8] P. Fosalba and E. Gaztanaga. Measurement of the gravitational potential evolution from the cross-correlation between WMAP and the APM Galaxy survey. *astro-ph/0305468*, 2003.
- [9] A. Gruzinov and W. Hu. "secondary cosmic microwave background anisotropies in a universe reionized in patches". *ApJ*, 508:435–439, Dec. 1998.
- [10] W. Hu. CMB temperature and polarization anisotropy fundamentals. *Annals of Physics*, 303:203–225, Jan. 2003.
- [11] W. Hu and M. White. "cmb anisotropies in the weak coupling limit.". *A&A*, 315:33–39, Nov. 1996.
- [12] W. H. Kinney. Inflation: Flow, fixed points, and observables to arbitrary order in slow roll. *Phys.Rev.D*, 66:83508+, Oct. 2002.
- [13] R. Knox, L. Scoccimarro and D. Dodelson. *Phys.Rev.Lett*, 81, 1998.
- [14] C. H. Lineweaver. "inflation and the cosmic microwave background. *Proceedings of the New Cosmology Summer School & astro-ph/0305179*, 2003.
- [15] J. P. Ostriker and E. T. Vishniac. Generation of microwave background fluctuations from non-linear perturbations at the era of galaxy formation. *ApJ*, 306:L51–L54, July 1986.
- [16] F. Pajot. PhD thesis, Paris VII University.
- [17] H. V. Peiris, E. Komatsu, L. Verde, D. N. Spergel, C. L. Bennett, M. Halpern, G. Hinshaw, N. Jarosik, A. Kogut, M. Limon, S. S. Meyer, L. Page, G. S. Tucker, E. Wollack, and E. L. Wright. First-Year Wilkinson Microwave Anisotropy Probe (WMAP) Observations: Implications For Inflation. *ApJS*, 148:213–231, Sept. 2003.
- [18] M. J. Rees and D. W. Sciama. Large scale density inhomogeneities in the universe. *Nature*, 217:511+, 1968.
- [19] R. K. Sachs and A. M. Wolfe. *ApJ*, 147:73, 1967.
- [20] U. Seljak. "rees-sciama effect in a cold dark matter universe". *ApJ*, 460:549+, Apr. 1996.

- [21] D. N. Spergel, L. Verde, H. V. Peiris, E. Komatsu, M. R.olta, C. L. Bennett, M. Halpern, G. Hinshaw, N. Jarosik, A. Kogut, M. Limon, S. S. Meyer, L. Page, G. S. Tucker, and E. Wollack. "first year wilkinson microwave anisotropy probe (wmap) observations: Determination of cosmological parameters". *Astrophys. J., in press & astroph/0302209*, 2003.
- [22] R. A. Sunyaev and I. B. Zeldovich. "the velocity of clusters of galaxies relative to the microwave background - the possibility of its measurement". *MNRAS*, 190:413–420, Feb. 1980.
- [23] R. A. Sunyaev and Y. B. Zeldovich. "formation of clusters of galaxies; protocluster fragmentation and intergalactic gas heating". *A&A*, 20:189+, Aug. 1972.
- [24] E. T. Vishniac. "reionization and small-scale fluctuations in the microwave background". *ApJ*, 322:597–604, Nov. 1987.
- [25] Y. B. Zeldovich and R. A. Sunyaev. *Astr. Sp. Sci.*, 4:301, 1969.